

Interactive social contagions and co-infections on complex networks

Quan-Hui Liu,^{1,2,3} Lin-Feng Zhong,^{1,2,4} Wei Wang,^{1,2,5,a)} Tao Zhou,^{1,2}
and H. Eugene Stanley⁴

¹Web Sciences Center, School of Computer Science and Engineering, University of Electronic Science and Technology of China, Chengdu 611731, China

²Big Data Research Center, University of Electronic Science and Technology of China, Chengdu 611731, China

³Laboratory for the Modeling of Biological and Socio-Technical Systems, Northeastern University, Boston, Massachusetts 02115, USA

⁴Center for Polymer Studies and Department of Physics, Boston, Massachusetts 02215, USA

⁵College of Computer Science and Technology, Chongqing University of Posts and Telecommunications, Chongqing 400065, China

(Received 22 October 2017; accepted 4 January 2018; published online 19 January 2018)

What we are learning about the ubiquitous interactions among multiple social contagion processes on complex networks challenges existing theoretical methods. We propose an interactive social behavior spreading model, in which two behaviors sequentially spread on a complex network, one following the other. Adopting the first behavior has either a synergistic or an inhibiting effect on the spread of the second behavior. We find that the inhibiting effect of the first behavior can cause the continuous phase transition of the second behavior spreading to become discontinuous. This discontinuous phase transition of the second behavior can also become a continuous one when the effect of adopting the first behavior becomes synergistic. This synergy allows the second behavior to be more easily adopted and enlarges the co-existence region of both behaviors. We establish an edge-based compartmental method, and our theoretical predictions match well with the simulation results. Our findings provide helpful insights into better understanding the spread of interactive social behavior in human society. *Published by AIP Publishing.*

<https://doi.org/10.1063/1.5010002>

Social contagion on complex networks has been studied for a long time, but they are limited to a single social spreading process. The phenomenon of adoption of one behavior impacting on adopting other behaviors occurs widely in the real world. The existing conclusions are not suitable to explain and the interactions among multiple social contagion processes also challenge the existing theoretical methods. To fill this gap, we try to purpose a model where two social behaviors sequentially spread on the same complex network. We, respectively, investigate the inhibitive effect and the synergistic effect of the adoption of first behavior on adopting the second behavior. Interestingly, both effects of the first behavior can change the phase transition type of the second behavior spreading. Therein, the inhibiting effect can cause the continuous phase transition of the second behavior spreading to become discontinuous. The synergistic effect can cause this discontinuous phase transition to become a continuous phase transition, which is a stark contrast to the synergy effect in two diseases interacting spreading. The results help us to obtain a deeper understanding of the interactions among multiple social contagion processes, and the developed theoretical method could also be applied to other analogous interactive dynamical processes.

I. INTRODUCTION

One spreading process simultaneously or sequentially interacting with other dynamical processes exists widely in the real world.^{1–3} Examples include concurrent infections with multiple pathogens,^{4–6} the simultaneous outbreak of the awareness of a disease and the disease itself,^{7–14} and memetic competition in media.^{15–18} When dynamical processes occur sequentially, such as seasonal influenza repeatedly returning to a population, one effect can be that individuals become less susceptible to future outbreaks when they acquire immunity from previous outbreaks.^{19,20} Similarly, in a social system, when a consumer has recently purchased an Android smart phone it lowers the probability that they will sometime soon purchase an iPhone. On the other hand, when they purchase a computer or smart phone, it increases the probability that they will also purchase apps or other software.^{21,22}

Recently, many researches have been done on interacting spreading phenomena in biological diseases. In terms of the interplay between the two interacting dynamical processes, this research falls into three categories: competitive,^{23–26} synergistic,^{27–35} and asymmetric.^{7–12} A model of two diseases spreading concurrently and competing for the same population of hosts is presented in Ref. 25. It found a coexistence regime in which both diseases can infect a substantial fraction of nodes in the network. For two diseases that synergistically spread simultaneously, Refs. 29 and 30 propose models in which a node infected by one disease

^{a)}wwzqbx@hotmail.com

becomes more susceptible to the other disease. Researchers have found that synergistic interaction can lead to explosive outbreaks of a disease and a discontinuous phase transition. As a further extension of Ref. 30, Cui *et al.* studied a susceptible-infected-removed-type model with two mutually cooperative pathogens on power-law networks; they found that the epidemic transition is discontinuous when cooperativity is sufficiently high for the network with a finite second moment of the degree distribution.³¹ In the control of disease spreading, models of asymmetrical interplay between the disease awareness and the disease are proposed in Refs. 7–12. They found that an awareness-based response suppresses the spread of disease, but does not cause the continuous phase transition to become discontinuous.

For studies on two subsequent spreading processes, most of them are about competing interactions in which an individual infected by a first disease becomes harder or cannot be infected by a second. A model of two diseases spreading one after the other on a single contact network is presented in Ref. 36. Researchers found a co-existence threshold above the classical epidemic threshold that indicates that two diseases can coexist. A study of two diseases successively spreading on overlay networks is presented in Ref. 37. The results showed that the network structure (e.g., the joint degree distribution and the edge overlap) and the strength of immunity strongly impact the parameter regions of possible coexistence, but that the immunity provided one disease does not change the type of phase transition. It also found that the final density of infection smoothly increases as the disease transmission rate increases. For other recent works, see Refs. 38 and 39.

In a social system, Ref. 40 uses two susceptible-infected-susceptible (SIS) spreading processes to study the exclusive and nonexclusive influences between two competing ideas. They find that the two ideas have multiple co-existences, and that the stationary densities of the ideas are determined primarily by their respective initial densities. The competition between an SIS spreading process and a threshold contagion process on an interdependent network has also been investigated.⁴¹ Researchers found that the continuous phase transition of the SIS spreading process can be changed to discontinuous one, and the discontinuous phase transition of the threshold contagion process can also be changed to a continuous phase transition with an asymmetry of intralayer connectivity. Very recently, the coevolution of internal activation and external activation in social dynamics is also investigated in complex networks, which displays rich phenomena, such as the hysteresis loop and the random switching between two coexisting states (opinions).^{42,43}

The key differences between biological and social contagions are the social reinforcement effect and non-Markovian properties,^{44,45} which are not considered in the existing studies about the interacting spreading dynamics.^{40,41} Specifically, the research about two interacting social contagion processes is rare, and there is no mathematical model that takes both inhibiting and synergistic effects into consideration. To fill this gap, we propose a model in which two interacting behaviors spread successively on a complex network. Each behavior is modeled by the

susceptible-adopted-recovered (SAR) non-Markovian spreading processes. The interactive mechanism is introduced as the adoption of the first behavior either allows or inhibits the spread of the second behavior. Our results indicate that introducing the inhibiting impact of the first behavior can change the continuous phase transition in the second behavior to discontinuous, and synergy from the first behavior can change a discontinuous phase transition in the second to continuous. This synergy from the first behavior also allows the second behavior to be more easily adopted, and it enlarges the co-existence region of both behaviors.

We organize this paper as follows. In Sec. II, we introduce the interacting social contagion model. In Sec. III, we develop the theory. In Sec. IV, we show the results of numerical simulation that are verified by the proposed theory. In Sec. V, we summarize our conclusions.

II. INTERACTING SOCIAL CONTAGION MODEL

Our model proposes two behaviors, behavior 1 and behavior 2, and they spread successively on a network. Behavior 1 is the first to spread and behavior 2 is the second. We use the generalized social contagion model proposed in Ref. 46 to describe the dynamical process of each behavior. During the spread of each behavior, i.e., behavior $b \in \{1, 2\}$, each node is susceptible (S), adopted (A), or recovered (R). When a node is in the susceptible state, it has not adopted behavior b . In an adopted state, the node has adopted behavior b and can transmit information about behavior b to neighbors. In the recovered state, the node has lost interest in transmitting information to its neighbors. Note that each susceptible node with property m records cumulative number of pieces of behavioral information that it receives from its adopted neighbors. The more pieces of behavioral information the susceptible node receives, the larger the probability that it will adopt the behavior, i.e., a social reinforcement effect.⁴⁷

To start the spread behavior 1, we randomly choose a seed to be in a behavior 1 adopted state and set the remaining nodes in the susceptible state. During each time step, the adopted node transmits information about behavior 1 (“information 1”) to each of its susceptible neighbors with an independent probability λ_1 . After the adopted node u successfully transmits information 1 to its susceptible neighbor v , it stops transmitting information 1 to neighbor node v , i.e., information transmission is non-redundant, and the total number of pieces of information 1 that node v possesses is increased by one. This new piece of information will cause node v to adopt behavior 1 with a probability

$$\pi(k, m) = 1 - (1 - \tau_1)^m, \quad (1)$$

where m is the cumulative number of pieces of information 1 that node v has received from adopted neighbors, τ_1 is the unit of adopting probability for each reception of information 1, and k is the degree of node v . Because node v can receive information 1 from multiple adopted neighbors during each time step, each time it receives information 1, it will attempt to adopt behavior 1. Here, if node u has received $m - 1$ pieces of information 1 and then receives the $(n + 1)$ -th

piece of information about behavior 1, it adopts behavior 1 with a probability $\pi(k, m + n)$. The model is necessarily a non-Markovian process, since the adopting probability depends on the memory which is quantified by the cumulative number of pieces of information. Each adopted node recovers with a probability γ_1 . The dynamical process of behavior 1 terminates when all adopted nodes have recovered. Denote variable X_u as the final state of each node u for behavior 1; $X_u = S$ means node u does not adopt behavior 1 and $X_u = R$ means node u has adopted behavior 1.

When the dynamical process of behavior 1 terminates, we randomly choose a seed node to be in the adopted state for behavior 2 and set the remaining nodes to be in the susceptible state for behavior 2. The spreading dynamics of behavior 2 are mathematically identical to the dynamics of behavior 1, except that the probabilities for transmission λ_2 and recovery γ_2 differ. In addition, when in this step, a susceptible node u of degree k and the X state for behavior 1 receives the p -th piece information 2 and the cumulative number of pieces of received information 2 is m , then node u adopts behavior 2 with a probability

$$\psi(k, m, X) = \begin{cases} 1 - (1 - \tau_2)^m, & X = S, \\ 1 - (1 - \alpha\tau_2)^m, & X = R, \end{cases} \quad (2)$$

where τ_2 is the unit adopting probability for each reception of information 2. The impact of adopting behavior 1 on the spread of behavior 2 is introduced. When a node has adopted behavior 1, i.e., when $X = R$, the actual unit adoption probability τ_2^a for this node for each reception of information 2 changes to $\tau_2^a = \alpha\tau_2$. The parameter α quantifies the strength of impact of the adoption of first behavior and is set in the range of $[0, 1/\tau_2]$, where $\alpha = 0$ indicates that when a node has adopted behavior 1, it never adopts behavior 2, and the maximum value $1/\tau_2$ indicates that a node that has adopted behavior 1 needs to receive only one piece of information 2 for it to adopt behavior 2. In addition, adopting behavior 1 inhibits the spread of behavior 2 when $\alpha \in [0, 1)$, and this impact becomes synergistic when $\alpha \in (1, 1/\tau_2]$. Adopting behavior 1 has no impact on adopting behavior 2 when $\alpha = 1$. The dynamical process terminates when all adopted nodes of behavior 2 have recovered.

III. EDGE-BASED COMPARTMENTAL THEORY

To describe the strong dynamical correlations among the states of neighbors in this model, we establish an edge-based compartmental approach inspired by Refs. 46 and 48–50. As described above, the dynamical processes of behavior 1 and behavior 2 differ in their dynamical parameters. Thus, we only need to derive the equations for behavior 1. Let $S_b(t)$, $A_b(t)$, and $R_b(t)$ be the fraction of the susceptible, adopted and recovered nodes of behavior $b \in \{1, 2\}$ at time t , respectively. When $t \rightarrow \infty$, $R_b(\infty)$ is the final adoption fraction of behavior b . For simplicity, we shorten $R_b(\infty)$ and $S_b(\infty)$ to R_b and S_b , respectively.

A. Dynamics of behavior 1

During the spread of behavior 1, node u is set to be in the cavity state,⁵¹ which means it can receive information 1 from its adopted neighbors but cannot transmit information 1 to its susceptible neighbors. Let $\theta_1(t)$ be the probability that a random neighbor v of node u has not transmitted information 1 to node u by time t . [The derivation of $\theta_1(t)$ is presented in the Appendix.] Thus, for a node u of degree k that is initially susceptible, the probability that node u has m pieces of information 1 at time t is $B_{k,m}[\theta_1(t)]$, where $B_{k,m}(w)$ is a binomial function of w that is equal to $\binom{k}{m} w^{k-m} (1-w)^m$. At time t , if node u is still in the susceptible state, it means that node u does not adopt behavior 1 at each reception of information 1. Thus, the probability that node u with cumulative m pieces of information is still in a susceptible state is $\prod_{i=0}^m [1 - \pi(k, i)]$. In addition, combining all possibilities of m , the probability that node u of degree k is still in the susceptible state at time t is

$$S_1(k, t) = \sum_{m=0}^k B_{k,m}(\theta_1(t)) \prod_{i=0}^m [1 - \pi(k, i)]. \quad (3)$$

Combining the degree of distribution $P(k)$ of the network, the fraction of susceptible nodes at time t is

$$S_1(t) = \sum_k P(k) S_1(k, t). \quad (4)$$

The fraction of adopted nodes $A_1(t)$ increases when susceptible nodes adopt behavior 1 and decreases when they recover, which also causes $R_1(t)$ to increase. Thus, the evolution equations for the fraction of adopted and recovered nodes of behavior 1 are

$$\frac{dA_1(t)}{dt} = -\frac{dS_1(t)}{dt} - \gamma_1 A_1(t) \quad (5)$$

and

$$\frac{dR_1(t)}{dt} = \gamma_1 A_1(t), \quad (6)$$

respectively. To solve Eqs. (3)–(6), we need to know $\theta_1(t)$, which can be written as

$$\begin{aligned} \frac{d\theta_1(t)}{dt} = & -\lambda_1 \theta_1(t) + \lambda_1 \frac{\sum_{k'} k' P(k') \Phi_1(k', \theta_1(t))}{\langle k \rangle} \\ & + \gamma_1 [1 - \theta_1(t)] (1 - \lambda_1), \end{aligned} \quad (7)$$

where $\Phi_1(k', \theta_1(t)) = \sum_{m=0}^{k'-1} B_{k'-1,m}(\theta_1(t)) \prod_{i=0}^m [1 - \pi(k', i)]$. We present derivations of Eq. (7) and $\Phi_1(k', \theta_1(t))$ in the Appendix. Using Eqs. (3)–(7), we can compute the fraction of each stated node at any time t .

The dynamical process of behavior 1 terminates when all the nodes adopting behavior 1 have recovered. Thus, there is no information 1 transmitted from the adopted node to its neighbors, which means that the right side of Eq. (7) is equal to zero when $t \rightarrow \infty$. For the sake of simplicity, we use θ_1 to represent $\theta_1(\infty)$, and Eq. (7) can be written as

$$\theta_1 = \frac{\sum_{k'} k' P(k') \Phi_1(k', \theta_1)}{\langle k \rangle} + \frac{\gamma_1(1 - \theta_1)(1 - \lambda_1)}{\lambda_1}. \quad (8)$$

Solving Eq. (8), we obtain the value of θ_1 and calculate the fraction of susceptible nodes S_1 by substituting θ_1 into Eqs. (3)–(4). The final adoption fraction of behavior 1 is $R_1 = 1 - S_1$.

For a fixed τ_1 , there is a critical value of λ_1 above which behavior 1 is widely adopted and below which it does not. We can obtain this critical value by determining when a non-trivial solution of Eq. (8) appears [$\theta_1 = 1$ is a trivial solution of Eq. (8)] as

$$g_1(\theta_1, \lambda_1) = \frac{\sum_{k'} k' P(k') \Phi_1(k', \theta_1)}{\langle k \rangle} + \frac{\gamma_1(1 - \theta_1)(1 - \lambda_1)}{\lambda_1} - \theta_1, \quad (9)$$

which is tangent to the horizontal axis at the critical value of θ_1^c . Thus, combining Eq. (8) and

$$\left. \frac{dg_1(\theta_1, \lambda_1)}{d\theta_1} \right|_{\theta_1^c} = 0, \quad (10)$$

we obtain the critical transmission rate of information 1 for fixed τ_1 .

B. Dynamics of behavior 2

In the above analysis, when the spread of behavior 1 terminates, the probability that a random node has adopted behavior 1 is approximately the final adoption size R_1 of behavior 1, and it correlates with θ_1 . For the sake of simplicity, let $\omega(X)$ be the probability of a random node with X state for behavior 1. Here, $X=S$ indicates that the node has not adopted behavior 1, and $X=R$ indicates that the node has adopted behavior 1, therein, $\omega(S) = 1 - R_1$ and $\omega(R) = R_1$. The actual unit adoption probability τ_2^a for each transmission of information 2 is based on whether the node has or has not adopted behavior 1. The probability $S_2(k, t)$ of a node u with degree k is still susceptible to behavior 2 at time t can be divided into two parts. The first is that node u has not adopted behavior 1 and does not adopt behavior 2 by time t . The second is that node u has adopted behavior 1 and does not adopt behavior 2 by time t . Similar to Eq. (3), we combine these two and write $S_2(k, t)$ as

$$S_2(k, t) = \sum_{X \in \{S, R\}} \omega(X) \sum_{m=0}^k B_{k,m} [\theta_2(t)] \times \prod_{i=0}^m [1 - \psi(k, i, X)], \quad (11)$$

where $\theta_2(t)$ is the probability that a random neighbor v of node u has not transmitted information 2 to u by time t . The fraction of susceptible nodes in the network for behavior 2 at time t is $S_2(t) = \sum_k P(k) S_2(k, t)$.

We replace $\pi(k', i)$ with $\psi(k', i, X)$ in Eq. (A2) and can obtain the probability $\Phi_2(k', \theta_1, \theta_2(t))$ that a neighbor node v of degree k' is susceptible to behavior 2. Substituting $\Phi_2(k', \theta_1, \theta_2(t))$ into Eq. (8), we obtain the final state of $\theta_2(t)$

$$\theta_2 = \frac{\sum_{k'} k' P(k') \Phi_2(k', \theta_1, \theta_2)}{\langle k \rangle} + \frac{\gamma_2(1 - \theta_2)(1 - \lambda_2)}{\lambda_2}, \quad (12)$$

and the function $g_2(\lambda_2, \theta_1, \theta_2)$ for behavior 2 is written as

$$g_2(\lambda_2, \theta_1, \theta_2) = \frac{\sum_{k'} k' P(k') \Phi_2(k', \theta_1, \theta_2)}{\langle k \rangle} + \frac{\gamma_2(1 - \theta_2)(1 - \lambda_2)}{\lambda_2} - \theta_2, \quad (13)$$

where θ_2 is the shortened notation for $\theta_2(\infty)$. Thus, for given λ_1 and λ_2 , we obtain the values of θ_1 and θ_2 by combining Eqs. (8) and (12). Substituting θ_1 and θ_2 into Eqs. (4) and (11), we obtain the final fraction of susceptible nodes S_2 , and the final adoption fraction of behavior 2 is $R_2 = 1 - S_2$.

Similar to the deviation in the critical transmission rate of information 1 for a given θ_1 (i.e., λ_1), we combine Eq. (12) and

$$\left. \frac{dg_2(\lambda_2, \theta_1, \theta_2)}{d\theta_2} \right|_{\theta_2^c} = 0, \quad (14)$$

to calculate the critical information transmission rate of behavior 2.

Note how the spread of behavior 1 affects the phase transition of R_2 on λ_2 , which can be analyzed by observing how θ_2 changes with λ_2 . Solving Eqs. (8) and (12), we obtain the relationship between θ_2 and λ_2 for different λ_1 , as shown in the top panel of Figs. 1 and 3. Here, $\theta_2 = 1$ is the trivial solution of Eq. (12), which indicates no spread of behavior 2. For $\alpha \in (0, 1)$, e.g., $\alpha = 0.5$, and $\lambda_1 = 0.2$, when we fix all parameters except λ_2 , Eq. (12) has only one root (i.e., a fixed point) for different values of λ_2 [Fig. 1(a)], and θ_2 smoothly decreases with λ_2 , which means that R_2 also smoothly increases with λ_2 . Figure 1(b) shows that when $\lambda_1 = 0.8$, the number of roots of Eq. (12) depends on λ_2 and the equation will have 3 roots for a range of λ_2 , which means that a saddle-node bifurcation occurs.⁵² When the equation has 3 roots, only the largest stable value is physically meaningful. When we vary λ_2 and cross its critical value (i.e., λ_{2c}^I), it jumps to its smallest roots, which means R_2 increases with λ_2 discontinuously [Fig. 1(b)]. It is the same for $\alpha \in (1, 1/\tau_2)$, e.g., $\alpha = 1.5$, as shown in Figs. 3(c) and 3(d). Thus, when we vary λ_1 (i.e., $\lambda_1 = 0.2$ and $\lambda_1 = 0.8$), it changes the phase transition of R_2 on λ_2 from continuous (discontinuous) to discontinuous (continuous) for the inhibition (synergy) effect of behavior 1, which means that the crossover phenomena in phase transition⁵³ exists in the system for both the inhibiting and synergetic effects of behavior 1. To determine the critical condition of the continuous (discontinuous) transition being changed to a discontinuous (continuous) transition in the inhibition (synergy) effect, we numerically solve Eqs. (12) and (14), and

$$\left. \frac{d^2 g_2(\lambda_2, \theta_1, \theta_2)}{d\theta_2^2} \right|_{\theta_2^c} = 0, \quad (15)$$

to obtain the critical θ_1^c value. Then, substituting θ_1^c into Eq. (8), we obtain the critical value of λ_1 . We denote λ_{2c}^H and λ_{2c}^I

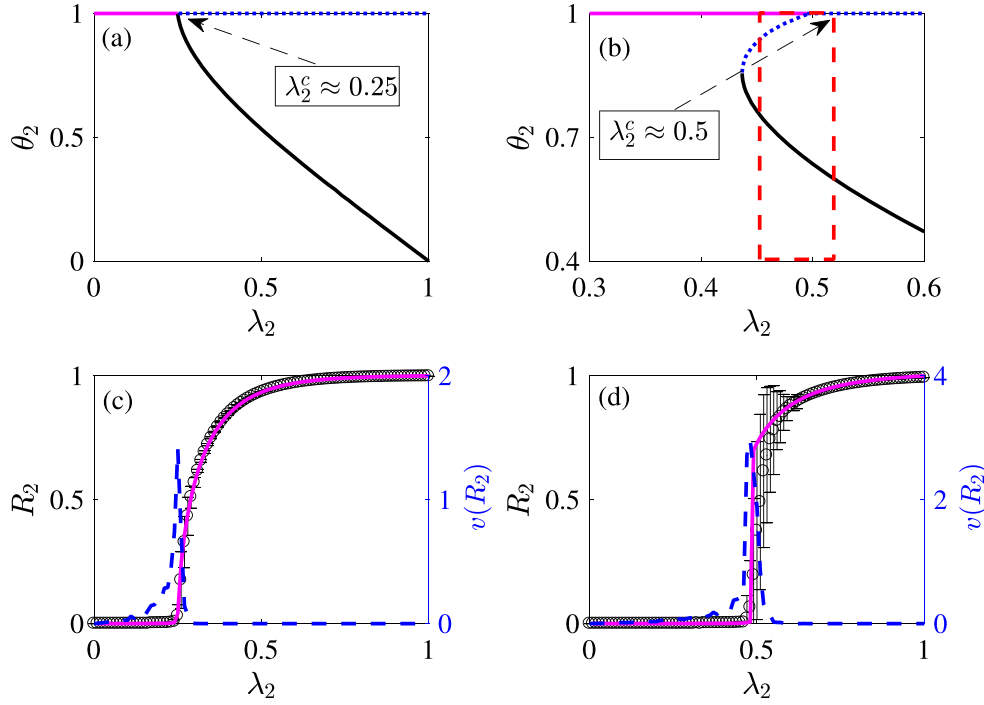


FIG. 1. Graphical analysis of θ_2 and the final adoption size of behavior 2 versus λ_2 with the inhibition effect (i.e., $\alpha = 0.5$) of first behavior on ER networks. (Top panel) The root of Eq. (12) versus λ_2 . As shown in (a) and (b), $\theta_2 = 1$ is the trivial solution of Eq. (12), therein, the solid lines represent the stable roots and the dotted lines represent the unstable roots. The parameters in (a) are $\lambda_1 = 0.2$, $\tau_1 = \tau_2 = 0.4$, and in (b) are $\lambda_1 = 0.8$, $\tau_1 = \tau_2 = 0.4$. (Bottom panel) The final adoption fraction R_2 (left coordinate) and the corresponding relative variance $v(R_2)$ (right coordinate) versus λ_2 . The parameters in (c) and (d), respectively, correspond to the parameters in (a) and (b). Therein, the black circles are the simulation results and the solid lines are the theoretical predictions. In (a), there is only one stable root for Eq. (12), thus R_2 increases with λ_2 continuously, as shown in (c). In Fig. 1(b) there is a region λ_2 , as shown in the rectangle, there are two stable roots for Eq. (12), but only the higher stable root is physically meaningful. When varying λ_2 crosses this region, it will make the physically meaningful root jumping to another smaller root. Thus, R_2 increases with λ_2 discontinuously, as shown in (d).

as the continuous and discontinuous critical information transmission rates of behavior 2 for R_2 on λ_2 , respectively.

IV. SIMULATION RESULTS

Here, we present simulation results and theoretical predictions, and study how the first behavioral adoption impacts the phase transition of R_2 on λ_2 and the coexistence region of both behaviors. We first perform simulations on the Erdős-Eényi (ER) network⁵⁴ and then, on a configuration network with a power-law degree distribution.⁵⁵ Unless otherwise specified, the network size and the network mean degree are, respectively, set to $N = 5 \times 10^4$ and $\langle k \rangle = 10$. The recovery probabilities for both behaviors are set to $\gamma_1 = 1.0$ and $\gamma_2 = 1.0$. We use at least 2×10^3 independent dynamical realizations on a fixed network to calculate the pertinent average values and further average them over 20 network realizations.

To identify the simulation threshold of information about behavior $b \in \{1, 2\}$, we employ a relative variance $v(R_b)$ method⁵⁶

$$v(R_b) = \frac{\langle R_b - \langle R_b \rangle \rangle^2}{\langle R_b \rangle^2}, \quad (16)$$

where $\langle \dots \rangle$ is the ensemble average and R_b the final adoption fraction of behavior b . Figures 1(c) and 1(d) and 3(c) and 3(d) show that $v(R_2)$ reaches a maximum value at the critical

information transmission rate (i.e., λ_{2c}^I and λ_{2c}^{II}) of behavior 2, which is the simulation threshold of behavior 2.

In Sec. IV B, we separately discuss the inhibiting effect and the synergistic effect of adopting first behavior on the spread of the second behavior on ER networks. And then, we present the simulation results of the two interacting behavior spreading on the network of power-law degree distribution.

A. Inhibiting effect of the first behavior on ER networks

A previous theoretical analysis of Eq. (12) found that the transmission rate λ_1 of information 1 impacts the type of phase transition of the second behavior. Here, we show that it also occurs in simulations and provide a qualitative explanation. For the adoption of behavior 1 inhibiting the spread of behavior 2, i.e., $\alpha < 1$, and the unit adopting probabilities set to $\tau_1 = 0.4$ and $\tau_2 = 0.4$, we find that the outbreak of behavior 1 will change the continuous phase transition of R_2 on λ_2 to discontinuous, as shown in the bottom panel of Fig. 1. When $\lambda_1 = 0.8$ (i.e., behavior 1 outbreaks), the actual unit probability τ_2^a for nodes that have adopted behavior 1 is decreased to $\alpha\tau_2 = 0.2$. The probabilities that these nodes (i.e., nodes that have adopted behavior 1) are still susceptible after receiving the first, second, and third pieces of information 2 are $1 - \psi(k, 1, R) = 0.8$, $[1 - \psi(k, 1, R)][1 - \psi(k, 2, R)] = 0.48$, and $[1 - \psi(k, 1, R)][1 - \psi(k, 2, R)][1 - \psi(k, 3, R)] = 0.192$, respectively. Compared to nodes with no pieces of information 2, these nodes easily adopt behavior 2, especially

when they have two or three pieces of information 2, i.e., when they experience the social enforcement effect.⁴⁷ A subcritical system state⁴⁶ for these susceptible nodes occurs when one node newly receiving a piece of information and adopting the behavior leads to an avalanche of behavior adoption. Suppose node u adopts behavior 2, transmits the information to neighbor v , and neighbor v adopts behavior 2 and with an independent probability λ_2 further transmits the information to its neighbors. This causes the nodes with two or three pieces of information 2 to also adopt behavior 2. This can lead to an abrupt behavioral adoption. Because there is a large fraction of nodes with two or three pieces of information 2, even a slight increase in the transmission suddenly and discontinuously increases R_2 with λ_2 , as shown in Fig. 1(d).

When $\lambda_1 = 0.2$, there is no outbreak of behavior 1, and its inhibition effect can be ignored. The fraction of subcritical susceptible nodes in the system is small since 40% [$\psi(k, 1, S) = 0.4$] of the nodes with one piece of information 2 will adopt behavior 2 and only 12% [$(1 - \psi(k, 2, S)) = 0.12$] nodes with two pieces of

information 2 are still susceptible. Thus, R_2 increases with λ_2 continuously, when there is no outbreak of behavior 1 (i.e., $\lambda_1 = 0.2$). The phase transition of R_2 on λ_2 is analyzed by the bifurcation theory⁵² [see Figs. 1(a) and 1(b)]. In addition, the inhibition effect causes the outbreak of behavior 1 to enlarge the critical information transition rate (i.e., λ_{2c}^I and λ_{2c}^{II}) of behavior 2. Figures 1(c) and 1(d) show that the theoretical predictions agree well with the simulation results.

In the above analysis, the spread of behavior 1 strongly impacts the adoption of behavior 2 and affects the type of phase transition, λ_{2c}^{II} and λ_{1c}^I . In the following, we examine how λ_1 and λ_2 affect R_2 for the inhibition effect of behavior 1. Figure 2 (top panel) shows that R_2 discontinuously increases with λ_2 and becomes more abrupt when λ_1 is increased above λ_{1c}^I . Note that an additional bifurcation analysis of Eq. (8) indicates that R_1 discontinuously increases with λ_1 when $\tau_1 = 0.3$, where λ_{1c}^I is the discontinuous critical information transmission rate of behavior 1. There is no outbreak of behavior 1, and R_2 discontinuously increases with λ_2 when $\tau_2 = 0.3$, which is proved by the

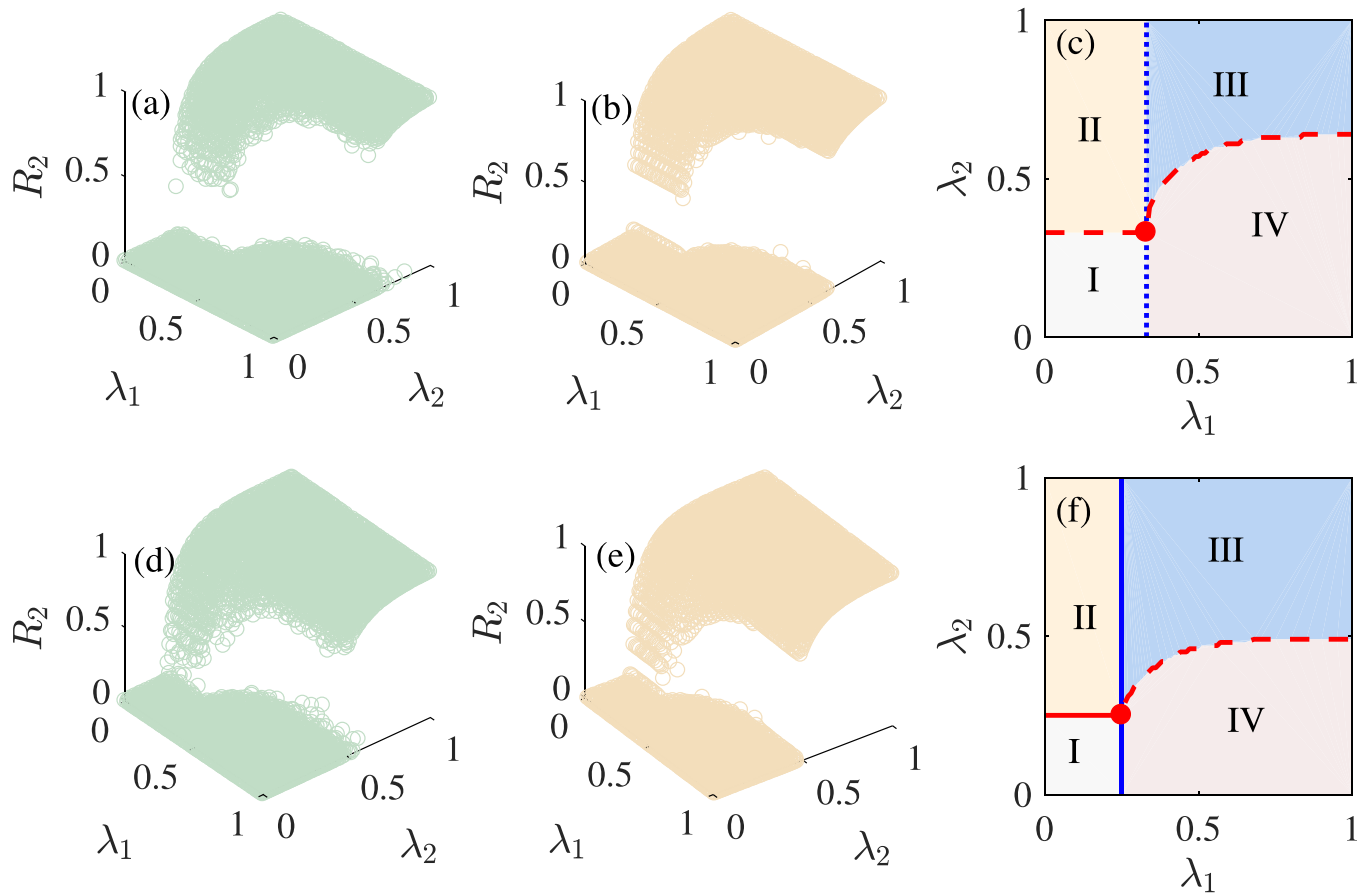


FIG. 2. The inhibition effect of behavior 1 on the spread of behavior 2 on ER networks. (a) The simulation results and (b) the theoretical predictions of the final adoption fraction R_2 on the plane (λ_1, λ_2) when the parameters are defined as $\alpha = 0.5, \tau_1 = 0.3, \tau_2 = 0.3$. (c) The phase diagram of the system. Region I represents no behaviors adopted and two behaviors are widely adopted in region III. Regions II and IV, respectively, represent only behavior 1 and only behavior 2, widely adopted. The blue vertical dotted line in (c) represents the discontinuous critical information transmission rate λ_{1c}^I of behavior 1 obtained by Eqs. (8) and (10). [It should be noted that the additional bifurcation analysis of Eq. (8) shows that R_1 increases with λ_1 discontinuously when $\tau_1 = 0.3$.] The red dashed line in (c) represents the critical information transmission rate λ_{2c}^I of behavior 2 [obtained by Eqs. (8), (12), and (14)]. The red circle is computed by Eqs. (8), (12), (14), and (15). Subfigures (d) and (f) are with the same meaning as subfigures (a)-(c), just with parameters $\alpha = 0.5, \tau_1 = 0.4, \tau_2 = 0.4$. The blue vertical solid line in (f) represents the continuous critical information transmission rate λ_{1c}^{II} of behavior 1 obtained by Eqs. (8) and (10). The red solid line and the red dashed line in (f) are, respectively, the λ_{2c}^{II} and λ_{2c}^I of behavior 2. The dotted and dashed lines in (c) and (f) represent crossing where R_2 (R_1) increases with λ_2 (λ_1) discontinuously. The solid lines in subfigures (c) and (f) represent crossing where R_2 (R_1) increases with λ_2 (λ_1) continuously.

bifurcation theory. When there is an outbreak of behavior 1, the unit adopting the probability of nodes that have adopted behavior 1 for each information 2 decreases; susceptible nodes need more pieces of information 2 to adopt the behavior, and so more nodes stay in the subcritical state. Thus, increasing λ_1 above λ_{1c}^I makes R_2 increase with λ_2 more abruptly and enlarges the outbreak information threshold λ_{2c}^I of behavior 2 [see the red dashed line in Fig. 2(c)]. There are four regions—I, II, III, and IV—in the plane (λ_1, λ_2) shown in Fig. 2(c). Region I is where there is no outbreak of either behavior when $\lambda_1 < \lambda_{1c}^I$ and $\lambda_2 < \lambda_{2c}^I$. Regions II and IV are where there is an outbreak of only behavior 2 and only behavior 1, respectively. Region III is the co-existence region in which there is an outbreak of both behaviors $\lambda_1 > \lambda_{1c}^I$ and $\lambda_2 > \lambda_{2c}^I$. It indicates that increasing λ_1 requires an increase in λ_2 to ensure that both behaviors coexist.

Figure 2 (bottom panel) shows that, when $\tau_2 = 0.4$, R_2 continuously increases with λ_2 when $\lambda_1 < \lambda_{1c}^{II}$. Note that an additional bifurcation analysis of Eq. (8) finds that R_1 increases with λ_1 continuously when $\tau_1 = 0.4$, and λ_{1c}^{II} is the continuous critical information transmission rate of behavior 1. The phase transition becomes discontinuous when there is an outbreak of behavior 1 (i.e., when

$\lambda_1 > \lambda_{1c}^{II}$), which is confirmed using bifurcation theory. As shown in Fig. 2(c), there are four regions in Fig. 2(f). In contrast to $\tau_2 = 0.3$ in Fig. 2(c), increasing τ_2 enlarges the co-existence region. The theoretical predictions agree well with the simulation results [see Figs. 2(a), 2(b), 2(e), and 2(f)].

B. Synergistic effect of the first behavior on ER networks

We study the synergy effect of behavior 1 on adopting behavior 2 in the following part. When the unit adopting probabilities for each information about both behaviors are set to 0.3 (i.e., $\tau_1 = 0.3$ and $\tau_2 = 0.3$), there is no outbreak of behavior 1 for $\lambda_1 = 0.2$. Thus the spread of behavior 1 has little impact on behavior 2. Nodes must receive more pieces of information 2 to adopt behavior 2 than when $\tau_2 = 0.4$. There are sufficient subcritical susceptible nodes in the system that increasing λ_2 slightly causes abrupt behavioral adoption. Figure 3(c) shows that R_2 increases with λ_2 discontinuously for $\lambda_1 = 0.2$. When there is an outbreak of behavior 1, i.e., $\lambda_1 = 0.8$, the synergy effect of behavior 1 causes the τ_2^q of nodes that have adopted behavior 1 for each information 2 to increase to $\alpha\tau_2 = 0.45$, which means that

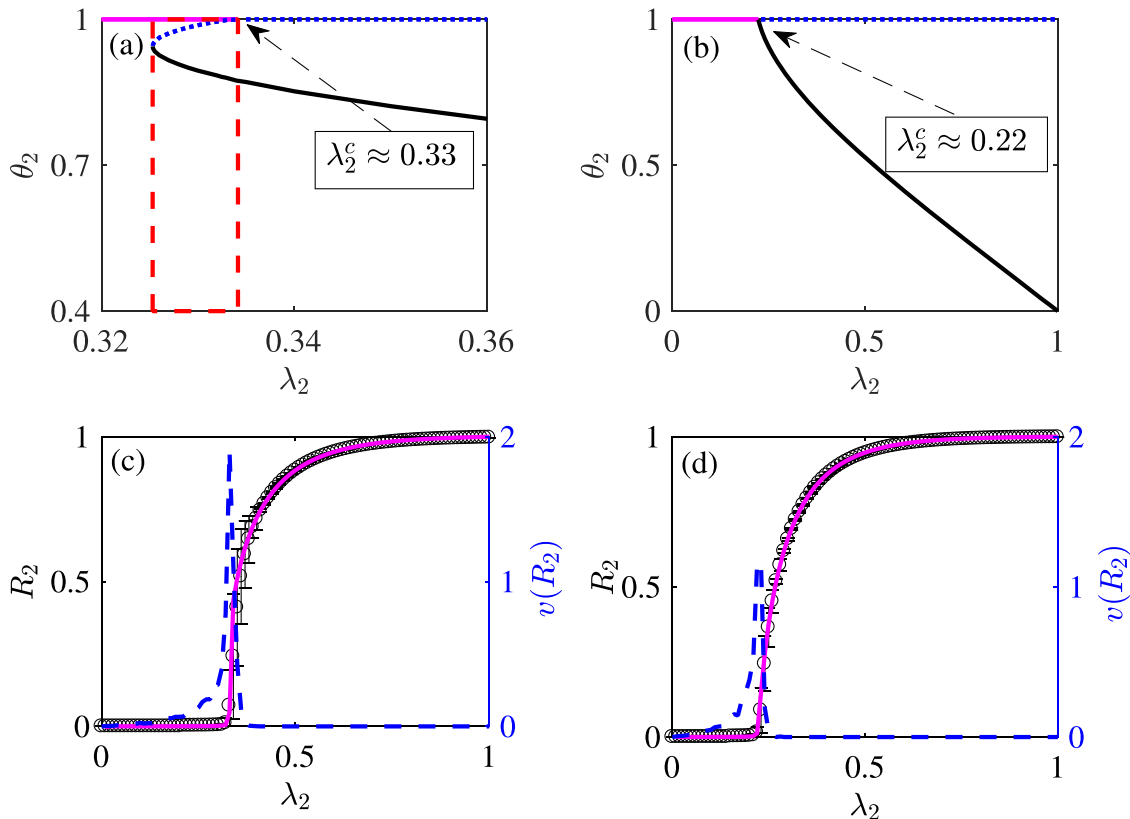


FIG. 3. Graphical analysis of θ_2 and the final adoption size of behavior 2 versus λ_2 with the synergy effect (i.e., $\alpha = 1.5$) of first behavior on ER networks. (Top panel) The root of Eq. (12) versus λ_2 . As shown in (a) and (b), $\theta_2 = 1$ is the trivial solution of Eq. (12), therein, the solid lines represent the stable roots and the dotted lines represent the unstable roots. The parameters in (a) are $\lambda_1 = 0.2$, $\tau_1 = \tau_2 = 0.3$, and in (b) are $\lambda_1 = 0.8$, $\tau_1 = \tau_2 = 0.3$. λ_{2c}^{II} and λ_{2c}^I , respectively, represent the continuous and discontinuous critical information transmission rates of behavior 2 for R_2 on λ_2 . (Bottom panel) The final adoption fraction R_2 (left coordinate) and the corresponding relative variance $v(R_2)$ (right coordinate) versus λ_2 . The parameters in (c) and (d), respectively, correspond to parameters in (a) and (b). Therein, the black circles are the simulation results and the solid lines are the theoretical predictions. In Fig. 3(a), there is a region of λ_2 , as shown in the rectangle, there are two stable roots for Eq. (12), but only the higher stable root is physical meaningful. When varying λ_2 crosses this region, it will make the physically meaningful root jumping to another smaller root. Thus, R_2 increases with λ_2 discontinuously, as shown in (c). In (b), there is only one stable root for Eq. (12); thus, R_2 increases with λ_2 continuously, as shown in (d).

approximately half of the nodes with one piece of information will adopt the behavior, and only the $[1 - \psi(k, 1, R)]$ $[1 - \psi(k, 2, R)] = 0.055$ fraction of these nodes is still in the susceptible state when they have received two pieces of information 2. The subcritical susceptible nodes (nodes with more than one piece of information 2) is very small. Thus, R_2 increases with λ_2 continuously when there is an outbreak of behavior 1, as shown in Fig. 3(d). Figures 3(a) and 3(b) show that the phase transition is proven by bifurcation theory. In addition, the synergy effect causes the outbreak of behavior 1 to decrease the critical transmission information rates (i.e., λ_{2c}^H and λ_{2c}^L) of behavior 2. Here, theoretical predictions also match the simulation results.

For the synergistic effect of behavior 1, we study the impact of λ_1 and λ_2 on the final adoption of behavior 2. For $\tau_2 = 0.3$, R_2 discontinuously increases with λ_2 when $\lambda_1 < \lambda_{1c}^I$, and becomes continuous when there is an outbreak of behavior 1 (i.e., when $\lambda_1 > \lambda_{1c}^I$), as shown in the top panel of Fig. 4. It shows a detailed analysis of the phase transition of R_2 on λ_2 , such as when $\lambda_1 = 0.2$ in Fig. 3(a) and when $\lambda_2 = 0.8$ in Fig. 3(b). There are also

four regions in Fig. 4(c). Region I is where there is no outbreak of either behaviors when $\lambda_1 < \lambda_{1c}^I$ and $\lambda_2 < \lambda_{2c}^L$. Regions II and IV are where there is an outbreak of only behavior 2 and only behavior 1, respectively. Region III is the co-existence region where there is an outbreak of both behaviors when $\lambda_1 > \lambda_{1c}^I$ and $\lambda_2 > \lambda_{2c}^H$. Compared with the inhibition effect of behavior 1, the synergy effect of behavior 1 makes the adoption of behavior 2 easier and enlarges the co-existence region of both behaviors [Fig. 4(c), region III].

When $\tau_2 = 0.4$, R_2 continuously increases with λ_2 and the synergy effect does not change the phase transition of R_2 in λ_2 . The unit adoption probability per information 2 for nodes having adopted behavior 1 is increased, which makes adopting behavior 2 easier. There are a few susceptible nodes in the subcritical state with two and three pieces of information 2. Thus, an outbreak of behavior 1 only decreases the outbreak threshold λ_{2c}^H of information 2 [red line in Fig. 4(f)]. At the same time, because of the synergy effect increasing τ_2 enlarges the co-existence region of both behaviors [region III in Fig. 4(f)].

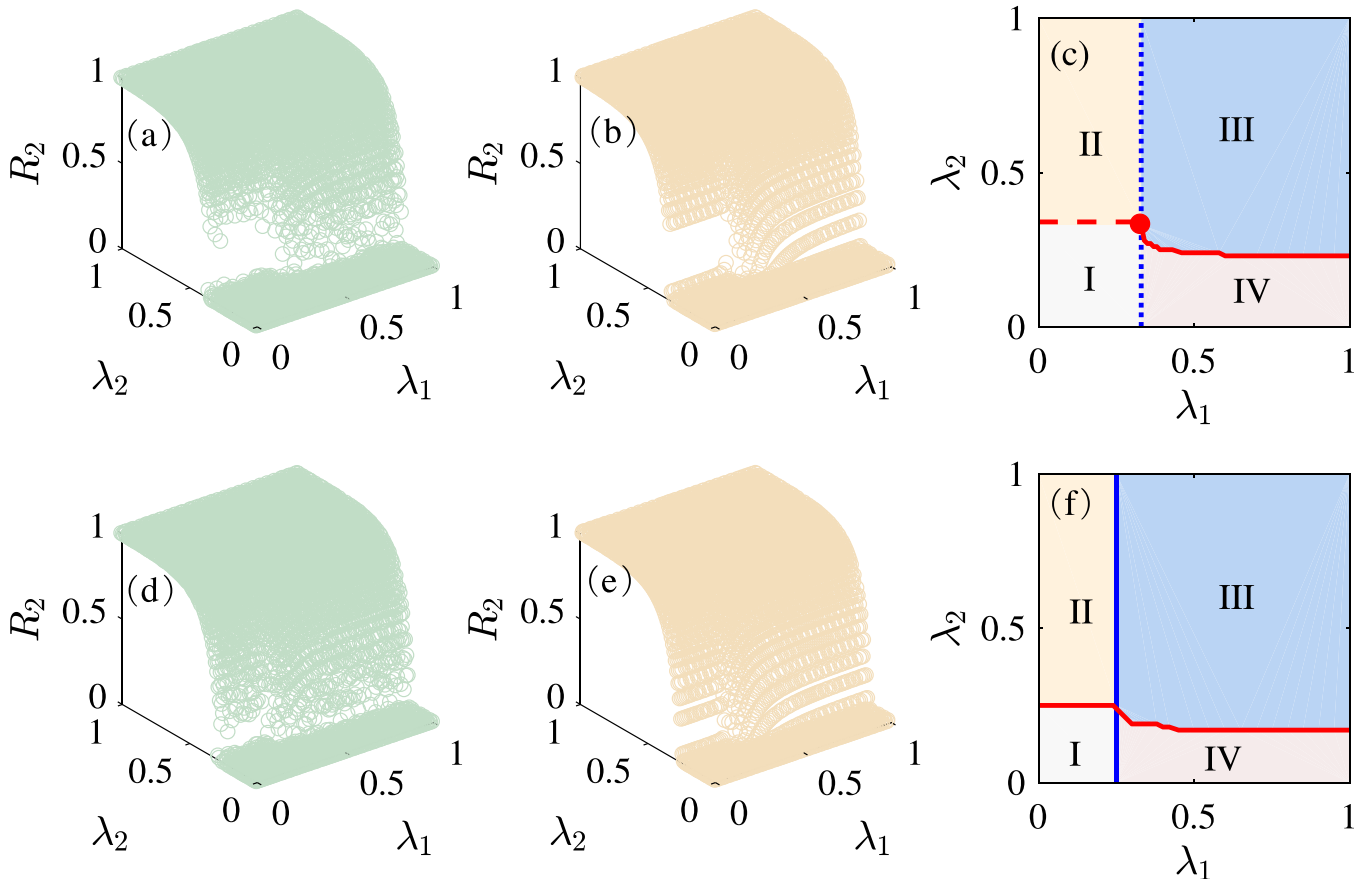


FIG. 4. The synergetic effect of behavior 1 on the spread of behavior 2 on ER networks. (a) The simulation results and (b) the theoretical predictions of the final adoption fraction R_2 on the plane (λ_1, λ_2) when the parameters are defined as $\alpha = 1.5$, $\tau_1 = 0.3$, $\tau_2 = 0.3$. (c) The two-dimensional plane through the phase diagram of the system. Region I represents no behaviors adopted, and two behaviors are widely adopted in region III. Regions II and IV, respectively, represent only behavior 1 and only behavior 2, widely adopted. The blue vertical dotted line in (c) represents the critical information transmission rate λ_{1c}^I of behavior 1 obtained by Eqs. (8) and (10). The red dashed line and the red solid line in (c), respectively, represent λ_{2c}^L and λ_{2c}^H of behavior 2 [obtained by Eqs. (8), (12), and (14)]. The red circle is computed by Eqs. (8), (12), (14), and (15). Subfigures (d) and (f) are with the same meaning as subfigures (a)–(c), just with parameters $\alpha = 1.5$, $\tau_1 = 0.4$, $\tau_2 = 0.4$. The blue solid line and the red solid line in (f), respectively, represent the critical information transmission rate λ_{1c}^I and λ_{2c}^H of behavior 1 and behavior 2. The dotted and dashed lines in (c) and (f) represent crossing, where R_2 (R_1) increases with λ_2 (λ_1) discontinuously. The solid lines in subfigures (c) and (f) represent crossing, where R_2 (R_1) increases with λ_2 (λ_1) continuously.

C. Two interacting behaviors spreading on scale-free networks

We also study the two behaviors sequentially spreading on scale-free networks,⁵⁷ constructed according to the standard configuration model.⁵⁵ The degree distribution is $P(k) = \Gamma k^{-\gamma}$, where γ is the degree exponent and $\Gamma = 1 / \sum_{k_{min}}^{k_{max}} k^{-\gamma}$ is the coefficient with $k_{min} = 3$ minimum degree, $k_{max} \sim N^{1/(\gamma-1)}$ maximum degree, and $\gamma = 3.0$. The network size and the mean degree of the network are set to $N = 5 \times 10^4$ and $\langle k \rangle = 10$, respectively. Figure 5 shows that when $\tau_1 = 0.3$ and $\tau_2 = 0.3$, R_2 smoothly increases with λ_2 when $\lambda_1 = 0.1$ (i.e., there is no outbreak of behavior 1). This continuous phase transition becomes discontinuous when it is inhibited by behavior 1 when it breaks out (e.g., when $\lambda_1 = 0.9$). When $\tau_1 = 0.08$ and $\tau_2 = 0.08$, the synergy effect of behavior 1 discontinuously increases R_2 with λ_2 when $\lambda_1 = 0.1$ (i.e., when there is no outbreak of behavior 1) and becomes a continuous phase transition when $\lambda_1 = 0.9$ (i.e., when there is an outbreak of behavior 1). The theoretical predictions match well with the simulation results.

V. CONCLUSIONS

We have studied two interactive behaviors sequentially spreading on an ER network. We find that with the outbreak of the first behavior, the inhibiting effect can cause the continuous phase transition of R_2 on λ_2 to become discontinuous. It can also enlarge spreading thresholds λ_{2c}^H and λ_{2c}^L of the second

behavior and decrease the co-existence region of both behaviors. The synergistic effect of the first behavior can make the discontinuous phase transition of the second behavior continuous. In addition, the threshold of information transmission rate for behavior 2 decreases and the synergistic effect of behavior 1 enlarges the co-existence region. Increasing the unit adopting probability of both information 1 and information 2 allows both the inhibition and synergy effects to make adoption of 2 easier and decreases λ_{2c}^H and λ_{2c}^L . We also develop an edge-based compartment method to describe how adopting the first behavior affects the spread of the second behavior. The theoretical predictions match the simulation results.

We simulate the spreading process on heterogeneous scale-free networks and verify the results with theoretical predictions. We find again that the continuous phase transition of R_2 on λ_2 can become discontinuous due to the inhibiting effect of the first behavior and that the synergistic effect of the first behavior can also cause the discontinuous phase transition of the second behavior to become continuous.

Our results indicate that prior behavioral adoption can produce a new phase transition and change the nature of pre-existing phase transitions in future behavioral adoption. They also explain why some behaviors spread rapidly and others very slowly. Further advances in the field could address the concurrent spreading of two or more dynamical processes and also how different transmitting paths differ in different spreading processes.

ACKNOWLEDGMENTS

This work was partially supported by the National Natural Science Foundation of China under Grant No. 61673086 and the program of China Scholarship Council (Grant Nos. 201606070059 and 201606070054).

APPENDIX: DERIVATION OF $\theta_1(t)$

For behavior 1, the model indicates that the neighbor of node u is in the susceptible, adopted, or recovered states, and we divide the calculation of $\theta_1(t)$ into three cases

$$\theta_1(t) = \zeta_1^S(t) + \zeta_1^A(t) + \zeta_1^R(t), \quad (A1)$$

where $\zeta_1^S(t)$ [$\zeta_1^A(t)$ or $\zeta_1^R(t)$] indicates that the susceptible (adopted or recovered) neighbor v of node u has not transmitted information 1 to u by time t . If the neighbor node v does not adopt behavior 1, it cannot transmit information 1. Thus, ζ_1^S is equal to the probability that a random neighbor v of node u is in the susceptible state at time t . When a random neighbor v of degree k' is initially susceptible, node u cannot transmit information 1 to v , and v receives only information 1 from other $k' - 1$ neighbors. The probability that node v has received m pieces of information 1 by time t is $B_{k'-1,m}[\theta_1(t)]$. Similar to the derivation of Eq. (3), the probability that node v is in the susceptible state is

$$\Phi_1(k', \theta_1(t)) = \sum_{m=0}^{k'-1} B_{k'-1,m}[\theta_1(t)] \prod_{i=0}^m [1 - \pi(k', i)]. \quad (A2)$$

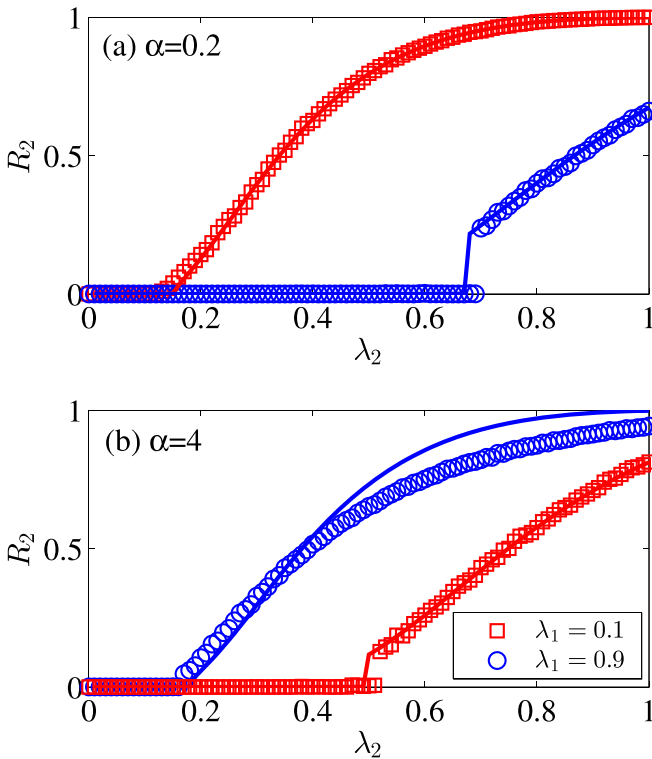


FIG. 5. Two behaviors sequentially spread on SF networks. (a) R_2 is versus λ_2 for the inhibition effect of behavior 1. Therein, $\tau_1 = 0.3$ and $\tau_2 = 0.3$. (b) R_2 is versus λ_2 for the synergy effect of behavior 1. Therein, $\tau_1 = 0.08$ and $\tau_2 = 0.08$. The lines with circles and squares are the simulation results and the solid lines are the theoretical predictions.

In an uncorrelated network, the probability that a random neighbor will have a degree k is $kP(k)/\langle k \rangle$. Thus, the probability that a random neighbor v of u is in the susceptible state is

$$\xi_1^S(t) = \frac{\sum_{k'} k' P(k') \Phi_1(k', \theta_1(t))}{\langle k \rangle}. \quad (\text{A3})$$

Here, $\xi_1^A(t)$ means that the adopted neighbor v of u has not transmitted information 1 to node u by time t . When node v succeeds in transmitting information 1 to node u , it decreases $\theta_1(t)$ to

$$\frac{d\theta_1(t)}{dt} = -\lambda_1 \xi_1^A(t). \quad (\text{A4})$$

When an adopted node recovers before it can transmit information 1 to its neighbors, $\xi_1^R(t)$ increases to

$$\frac{d\xi_1^R(t)}{dt} = \gamma_1(1 - \lambda_1)\xi_1^A(t). \quad (\text{A5})$$

Combining Eqs. (A4) and (A5), we obtain

$$\xi_1^R(t) = \frac{\gamma_1[1 - \theta_1(t)](1 - \lambda_1)}{\lambda_1}. \quad (\text{A6})$$

Inserting Eqs. (A3) and (A6) into Eq. (A1), we obtain

$$\begin{aligned} \xi_1^A(t) = \theta_1(t) - \frac{\sum_{k'} k' P(k') \Phi_1(k', \theta_1(t))}{\langle k \rangle} \\ - \frac{\gamma_1[1 - \theta_1(t)](1 - \lambda_1)}{\lambda_1}. \end{aligned} \quad (\text{A7})$$

Substituting Eq. (A7) into Eq. (A4), we obtain the time evolution of $\theta_1(t)$

$$\begin{aligned} \frac{d\theta_1(t)}{dt} = -\lambda_1 \theta_1(t) + \lambda_1 \frac{\sum_{k'} k' P(k') \Phi_1(k', \theta_1(t))}{\langle k \rangle} \\ + \gamma_1[1 - \theta_1(t)](1 - \lambda_1). \end{aligned}$$

¹A. Barrat, M. Barthélemy, and A. Vespignani, *Dynamical Processes on Complex Networks* (Cambridge University Press, 2008).

²A. Vespignani, *Nat. Phys.* **8**, 32 (2012).

³R. Pastor-Satorras, C. Castellano, P. Van Mieghem, and A. Vespignani, *Rev. Mod. Phys.* **87**, 925 (2015).

⁴J. K. Taubenberger and D. M. Morens, *Emerging Infect. Dis.* **12**, 15–22 (2006).

⁵J. F. Brundage and G. Shanks, *Emerging Infect. Dis.* **14**, 1193 (2008).

⁶S. Gomez, A. Diaz-Guilera, J. Gomez-Gardenes, C. J. Perez-Vicente, Y. Moreno, and A. Arenas, *Phys. Rev. Lett.* **110**, 028701 (2013).

⁷S. Funk, E. Gilad, C. Watkins, and V. A. Jansen, *Proc. Natl. Acad. Sci. U. S. A.* **106**, 6872 (2009).

⁸C. Granell, S. Gómez, and A. Arenas, *Phys. Rev. Lett.* **111**, 128701 (2013).

⁹C. Granell, S. Gómez, and A. Arenas, *Phys. Rev. E* **90**, 012808 (2014).

¹⁰W. Wang, M. Tang, H. Yang, Y. Do, Y. C. Lai, and G. Lee, *Sci. Rep.* **4**, 5097 (2014).

¹¹Q. H. Liu, W. Wang, M. Tang, and H. F. Zhang, *Sci. Rep.* **6**, 25617 (2016).

¹²W. Wang, Q. H. Liu, S. M. Cai, M. Tang, L. A. Braunstein, and H. E. Stanley, *Sci. Rep.* **6**, 29259 (2016).

¹³G. Ferraz de Arruda, E. Cozzo, T. P. Peixoto, F. A. Rodrigues, and Y. Moreno, *Phys. Rev. X* **7**, 011014 (2017).

¹⁴Y. Moreno, R. Pastor-Satorras, and A. Vespignani, *Eur. Phys. J. B* **26**, 521 (2002).

¹⁵J. P. Gleeson, J. A. Ward, K. P. O'sullivan, and W. T. Lee, *Phys. Rev. Lett.* **112**, 048701 (2014).

¹⁶M. Coscia, *Ann. Univ. Ferrara* **59**, 1 (2013).

¹⁷X. Wei, C. Nicholas, B. A. Prakash, I. Neamtii, M. Faloutsos, and C. Faloutsos, *IEEE J. Sel. Areas Commun.* **31**, 1049 (2013).

¹⁸L. Weng, A. Flammini, A. Vespignani, and F. Menczer, *Sci. Rep.* **2**, 335 (2012).

¹⁹M. I. Nelson and E. C. Holmes, *Nat. Rev. Genet.* **8**, 196 (2007).

²⁰C. A. Russell, T. C. Jones, I. G. Barr, N. J. Cox, R. J. Garten, V. Gregory *et al.*, *Science* **320**, 340 (2008).

²¹E. J. M. Arruda-Filho, J. A. Cabusas, and N. Dholakia, *Int. J. Inf. Manage.* **30**, 475 (2010).

²²F. Aldhaban, in *Proceedings of the Technology Management for Emerging Technologies* (2012), pp. 2758–2770.

²³J. Sanz, C. Y. Xia, S. Meloni, and Y. Moreno, *Phys. Rev. X* **4**, 041005 (2014).

²⁴J. C. Miller, *Phys. Rev. E* **87**, 060801 (2013).

²⁵B. Karrer and M. E. J. Newman, *Phys. Rev. E* **84**, 036106 (2011).

²⁶F. D. Sahneh and C. Scoglio, *Phys. Rev. E* **89**, 062817 (2014).

²⁷M. Martcheva and S. S. Pilyugin, *SIAM J. Appl. Math.* **66**, 843 (2006).

²⁸L. Chen, F. Ghanbarnejad, W. Cai, and P. Grassberger, *EPL* **104**, 50001 (2013).

²⁹L. Hébert-Dufresne and B. M. Althouse, *Proc. Nat. Acad. Sci. U. S. A.* **112**, 10551 (2015).

³⁰W. Cai, L. Chen, F. Ghanbarnejad, and P. Grassberger, *Nat. Phys.* **11**, 936 (2015).

³¹P.-B. Cui, F. Colaiori, and C. Castellano, *Phys. Rev. E* **96**, 022301 (2017).

³²N. Azimi-Tafreshi, *Phys. Rev. E* **93**, 042303 (2016).

³³P. Grassberger, L. Chen, F. Ghanbarnejad, and W. Cai, *Phys. Rev. E* **93**, 042316 (2016).

³⁴Q. H. Liu, W. Wang, M. Tang, T. Zhou, and Y. C. Lai, *Phys. Rev. E* **95**, 042320 (2017).

³⁵Y. Zha, T. Zhou, and C. Zhou, *Proc. Nat. Acad. Sci. U. S. A.* **113**, 14627 (2016).

³⁶M. E. J. Newman, *Phys. Rev. Lett.* **95**, 108701 (2005).

³⁷S. Funk and V. A. Jansen, *Phys. Rev. E* **81**, 036118 (2010).

³⁸M. E. J. Newman and C. R. Ferrario, *PLoS One* **8**, e71321 (2013).

³⁹L. G. A. Zuzek, H. E. Stanley, and L. A. Braunstein, *Sci. Rep.* **5**, 12151 (2015).

⁴⁰Y. Wang, G. Xiao, and J. Liu, *New J. Phys.* **14**, 013015 (2012).

⁴¹A. Czaplicka, R. Toral, and M. San Miguel, *Phys. Rev. E* **94**, 062301 (2016).

⁴²L. Böttcher, J. Nagler, and H. J. Herrmann, *Phys. Rev. Lett.* **118**, 088301 (2017).

⁴³L. Böttcher, M. Luković, J. Nagler, S. Havlin, and H. J. Herrmann, *Sci. Rep.* **7**, 41729 (2017).

⁴⁴P. S. Dodds and D. J. Watts, *Phys. Rev. Lett.* **92**, 218701 (2004).

⁴⁵A. Banerjee, A. G. Chandrasekhar, E. Duflo, and M. O. Jackson, *Science* **341**, 1236498 (2013).

⁴⁶W. Wang, M. Tang, H. F. Zhang, and Y. C. Lai, *Phys. Rev. E* **92**, 012820 (2015).

⁴⁷L. Lü, D. B. Chen, and T. Zhou, *New J. Phys.* **13**, 123005 (2011).

⁴⁸J. C. Miller, A. C. Slim, and E. M. Volz, *J. R. Soc., Interface* **9**, 890 (2012).

⁴⁹W. Wang, M. Tang, P. Shu, and Z. Wang, *New J. Phys.* **18**, 013029 (2016).

⁵⁰W. Wang, M. Tang, H. E. Stanley, and L. A. Braunstein, *Rep. Prog. Phys.* **80**, 036603 (2017).

⁵¹B. Karrer and M. E. J. Newman, *Phys. Rev. E* **82**, 016101 (2010).

⁵²S. H. Strogatz, *Nonlinear Dynamics and Chaos: With Applications to Physics, Biology, Chemistry and Engineering* (Westview, Boulder, CO, 1994).

⁵³S. N. Dorogovtsev, A. V. Goltsev, and J. F. Mendes, *Rev. Mod. Phys.* **80**, 1275 (2008).

⁵⁴P. Erdős and A. Rényi, *Publ. Math.* **6**, 290–297 (1959).

⁵⁵M. Catanzaro, M. Boguñá, and R. Pastor-Satorras, *Phys. Rev. E* **71**, 027103 (2005).

⁵⁶W. Chen, M. Schröder, R. M. D'Souza, D. Sornette, and J. Nagler, *Phys. Rev. Lett.* **112**, 155701 (2014).

⁵⁷M. E. J. Newman, *Phys. Rev. E* **66**, 016128 (2002).